Observations and a Geometric Explanation of the Effects of Humic Acid on Flocculation

A Thesis
Presented to the Faculty of the Graduate School
of Cornell University
In Partial Fulfillment of the Requirements for the Degree of
Master of Science

by

Yingda Du

December 2017

ABSTRACT

Natural organic matter (NOM) is found in all surface, ground and soil waters. NOM in water has a significant effect on drinking water treatment. The presence of NOM can create a need for increased coagulant doses in drinking water treatment. Humic and fulvic materials represent up to 70% of dissolved organic carbon (DOC) and are major components of NOM. This work evaluated the effect of humic acids on the particle size distribution of flocs and settled effluent turbidity for a synthetic surface water treated with polyaluminum chloride (PACl) as coagulant. Results obtained from this study indicate that the presence of NOM increased the concentration of flocs and shifted the particle size distribution toward smaller particle sizes with a concurrent increase in the effluent turbidity. A mechanistically based hydraulic flocculation model, which takes effects of humic acids into account, was developed in this research based on observations of residual turbidity. The model was validated by successfully predicting data from independent experiments. The predictive model provides a useful guideline for effective coagulant dosages in water treatment.

BIOGRAPHICAL SKETCH

Yingda Du was born in Loudi, China in 1993. She graduated with a degree in Environmental Engineering from Naikai University in 2015. In the Junior year, she had studied the effectiveness of Nitrobacteria as a treatment agent on high ammonia-nitrogen wastewater under the guidance of professor Dongfang Liu. In the summer before her senior year, she had an internship in Shenzhen Institute of Building Research working on testing results for the purpose of developing a website to educate the public on most suitable water purifier for specific types water. During the senior year, she conducted research on the toxic effects of graphene oxide on plants advised by Professor Xiangang Hu. In September 2015, she entered Cornell University and started her study towards the M.S. Degree in Environmental Engineering.

ACKNOWLEDGMENTS

Firstly, I would like to thank Dr. Monroe Weber-Shirk and Dr. Len Lion for their guidance and encouragement in the research. I count myself among the very fortunate to be able to call them my advisors and mentors. My growth as a student, engineer, and researcher during my time in graduate school is due, in large part, to their guidance. I acknowledge the inspirational instruction of Dr. Monroe Weber-Shirk. He has spent considerable time teaching me and guiding the research. I would like to thank Dr. Len Lion for his support, patience, and reassurance as I moved through the process of experiments and writing. I would also like to thank Dr. Damian Helbling who served as the minor advisor in the committee.

I am grateful to Casey Garland, William Pennock, two graduate students in the lab for their practical suggestions, conversation and technical support. I am also grateful to Karen Swetland, whom I have never met, but whose academic footsteps I am following.

TABLE OF CONTENTS

LIST OF FIGURES

LIST OF TABLES

LIST OF ABBREVIATIONS

NTU	Nephelometric Turbidity Unit
PACl	Polyaluminum chloride
NOM	Natural Organic Matter
HA	Humic acid
DOC	Dissolved Organic Carbon
DOM	Dissolved Organic Matter

LIST OF SYMBOLS

C_{clay}	clay concentration added to raw water
$C_{effluent}$	fraction of the effluent turbidity caused by the floc size class
$C_{influent}$	influent turbidity
C_{plant}	Al dose within the flocculator
D	inner diameter of the flocculator tube
D_{Clay}	diameter of clay particle
D_{FOV}	depth of field of view
d_p	the diameter of a particle
d_{HA}	diameter of humic acid molecule;
d_{PACI}	diameter of precipitated coagulant particle.
$\overline{G}$	average velocity gradient
H_{FOV}	length of field of view
k	model fitting parameter
N_{image}	number of images collected
N_{HA}	number concentration of humic acid macromolecules
N_{PACI}	is the number concentration of coagulant nanoparticles
$N_{particle}$	number of identified particles from the collected images
ρ_{PACI}	density of the coagulant

Q_{plant} experimental flow rate

R_c diameter of curvature of the flocculator coils

T camera shutter time

v_{flow} flow velocity through the image analysis system

V_{Clay} volume of a clay platelet

$V_{monitored}$ volume of water monitored for each experiment

V_{FOV} height of field of view

Γ fractional surface coverage of colloidal particle

$\Gamma_{HAtoCoag}$ coverage of coagulant surface by humic acid,

$\Gamma_{CoagToClay}$ fractional surface coverage of particle by coagulant,

θ flocculation resident time,

α attachment efficiency

$\alpha_{Clay-PACl}$ attachment efficiency between clay particle surface and a PACl surface of a PACl-HA nanoaggregate

$\alpha_{PACl-PACl}$ attachment efficiency between two PACl surface of a PACl-HA nanoaggregate

$\alpha_{PACl-HA}$ attachment efficiency between a PACl surface of a PACl-HA nanoaggregate and a HA surface of a PACl-HA nanoaggregate

v kinematic viscosity of fluid

Λ average separation distance between particles

ε average energy dissipation rate

ϕ	floc volume fraction
pC^*	turbidity removal efficiency

CHAPTER 1: INTRODUCTION

This research contributed to the AguaClara program at Cornell University. AguaClara is a multi-disciplinary program that designs sustainable water treatment systems. Research in the program supports electricity-free and locally-sourced water treatment technologies. The resulting technology is scalable to fit the needs of communities with populations between 1,500 and 25,000. Approximately 50,000 people in Honduras are currently served by water treatment systems designed using AguaClara technologies (AguaClara, 2017).

The research in this thesis explores the effects of natural organic matter (NOM) on flocculation. Flocculation facilitates aggregation of particles at drinking water treatment plants and is a crucial pretreatment step prior to particle removal by sedimentation and filtration. NOM is found in all surface, and ground waters and has a significant effect on drinking water treatment, especially on flocculation processes. NOM is complex mixture of molecules with varying molecular weight, chemical nature, and originates from a variety of sources. In this research, humic acid was chosen as an experimental surrogate for NOM and kaolin clay was utilized as an experimental surrogate for colloidal solids.

There are two major parameters used to determine the effectiveness of flocculation. One is the particle size distribution of flocs formed in the flocculation process and the other is settled effluent turbidity. As flocculation is heavily dependent on the chemical nature of the water being treated, the particle size distribution of flocs

and effluent turbidity are affected by the concentration of NOM in the system. Knowledge of how the NOM affects floc formation is limited. A better understanding of how NOM affects flocculation is needed to inform the development of a robust flocculation/sedimentation/filtration treatment process sequence scheme.

The main objective of this research was to explore the effect of humic acid on flocculation. It was hypothesized that variation in humic acid concentration in water would result in differences in the floc size distribution and settled effluent turbidity. In this thesis, chapter 2 presents the development of a flocculation model incorporating the effects of humic acid, and chapter 3 shows the observations of the effects of humic acid on particle size after flocculation. Chapter 4 summarizes results and suggests further work to expand the ability to model flocculation and study particle size distributions after flocculation with the influence of humic acid.

CHAPTER 2: DEVELOPMENT OF A FLOCCULATION/SEDIMENTATION MODEL WITH CONSIDERATION OF THE EFFECTS OF HUMIC ACID*

2.1 Abstract

Natural organic matter (NOM) is found in all surface, and ground waters. NOM in water has a significant effect on drinking water treatment (Matilaininen and Sillanpaa, 2010), since the presence of NOM can creaate a need for increased coagulant doses. This work evaluated use of polyaluminum chloride (PACI) as a coagulant for a synthetic surface water to determine the effect of NOM on the settled effluent turbidity. Mechanistically based scalable algorithms for operation of hydraulic flocculators were developed in this research based on observations of residual turbidity when kaolin clay and varying concentrations of humic acid were used to create synthetic raw water. Data were obtained using a laminar-flow tube flocculator and quiescent settling column. The research employed a previously published flocculation model (Swetland, et al. 2014) and considered modifications to the model algorithm to incorporate the effects of humic acid. Two adjustable model parameters were used to fit data. The modified model that accounted for the presence of humic acid was able to independently predict the experimental results from 60 experiments at a different influent turbidity. The predictive model is expected to be a useful tool to estimate the coagulant cost based on humic acid concentration and inflow turbidity in water treatment plant operation.

* This chapter will be submitted to a peer-review journal with co-authors Leonard Lion and Monroe Weber-Shirk

2.2 Introduction

The main objective of this research was to observe and model the effects of humic acids on flocculation to enhance the performance of a flocculator in the context of process train with subsequent unit processes (e.g., sedimentation and filtration) while minimizing operation costs. Prior research has shown that multiple variables influence the performance of hydraulic flocculators in drinking water treatment, including the concentration and type of colloids in the raw water, the concentration of dissolved organic matter, coagulant type and dose, and hydraulic residence time and energy dissipation rate in the flocculator (Kawamura, 1991).

The design and operation of hydraulic flocculators would be assisted by a predictive model that can characterize performance of alternative designs. An early model developed by Camp (1955) included $G\theta$ as a measure of flocculation, where G is the fluid velocity gradient and is proportional to the rate of colloid collisions, and θ is the time over which collisions occur. Based on this concept, Ives (1968) and O'Melia (1972) refined the model to include the floc volume fraction (Φ) and attachment efficiency (α). A general scalable model which uses dimensionally correct relationships that are based upon relevant flocculation mechanisms was created by Swetland, et al. (2014) and successfully applied to quantify the effect of varying flocculator design and operational parameters on the post-sedimentation residual turbidity that corresponded to a selected sedimentation capture velocity. This model did not account for the presence of varying levels of dissolved organic matter.

Humic acid is one of the major components of natural organic matter (NOM) that is found in all surface, ground and soil waters and has a significant effect on drinking water treatment, especially on flocculation processes. Quantifying the effect of varying flocculator design and operational parameters on settled effluent turbidity in the treatment of raw waters containing significant NOM concentrations would be an instructive improvement in flocculation design and operation.

Jarvis and Jefferson state that the aggregation mechanisms through which NOM is removed include a combination of change neutralization, entrapment, adsorption and complexation with coagulant metal ions into insoluble particulate aggregates (2007). Optimal conditions for turbidity or pathogen removal are not always the same as those for NOM removal (Hua and Reckhow, 2008). Because of the variable composition of NOM, the mechanisms of removal could be different for different types of NOM in water (Sharp and Jarvis, 2006). The flocs formed through different mechanisms would result in a variation of physical properties such as size, structure, and strength (Amin et al., 2012). The effectiveness of flocculation for removal of NOM depends on many factors, including pH, temperature, particle and NOM properties, coagulant type and dosage, as well as the presence of divalent cations and concentrations of destabilizing anions. The nature of NOM has a significant effect on the coagulant dosage, and the hydrophobic fraction of NOM is generally removed in coagulation more effectively than the hydrophilic fraction. (Matilainen and Vepsalainen, 2010).

Increasing the alum dose has been shown to increase NOM removal up to a certain point; however, NOM removal is not significantly improved when adding very high alum dosages (> 100 mg/L), which suggests that some components of NOM are

recalcitrant to being removed by coagulant (Soh 2008; Chow 2009). Solution pH has a significant effect on coagulation efficiency, and optimal pH is in the range of 5.0- 6.5 for the alum coagulant ((Matilainen and Vepsalainen, 2010). Prehydrolyzed polymer coagulants have been reported to have advantages over conventional coagulants such as alum, including less temperature or pH dependence, as well as smaller alkalinity consumption, but the characteristics of the water to be treated (e.g. alkalinity, pH, and NOM content) play a major role in the choice of a proper coagulant. Consequently, prehydrolyzed coagulants have not been consistently observed to enhance the removal efficiency of NOM (Hu 2006).

The research described herein builds on the Swetland, et al. (2014) flocculation model and adds detail to the attachment efficiency term describing geometric and probabilistic interactions between clay, coagulant, NOM, and reactor walls. The synthetic raw water used in experiments added one type of NOM to a previously studied synthetic system (Swetland et al, 2014) in the hope that the resulting system would be sufficiently well characterized to develop a predictive model.

The Swetland model is based on the observation that PACl precipitates form nanoparticles that attach to clay and reactor wall surfaces. Swetland et al. (2014) found particle attachment efficiency in a hydraulic flocculator to be proportional to the fractional surface coverage of suspended clay by precipitated coagulant (alum and polyaluminum chloride (PACl)) nanoparticles. The success of the surface coverage model to explain the interactions between clay, coagulant nanoparticles, and reactor walls led to the hypothesis that NOM nanoparticles may attach to the coagulant nanoparticles and reduce the amount of surface area that is available for attachment.

2.3 Experimental Methods

Experiments were conducted using the laboratory apparatus illustrated in figure 1. Cornell University tap water was pumped from a temperature-controlled reservoir and mixed with a concentrated stock suspension of kaolinite clay (R.T. Vanderbilt Co., Inc) to form a feed-back regulated constant turbidity raw water source (Weber-Shirk, 2008). Reported Cornell University tap water characteristics are as follows: total hardness ≈150 mg/L as $CaCO_3$; total alkalinity ≈108 mg/L as $CaCO_3$; pH ≈ 7.44; turbidity ≈ 0.06 nephelometric turbidity units (NTU); and dissolved organic carbon ≈1.95 mg/L (Bolton Point Water System 2015). A concentrated stock of suspension of humic acids was then mixed with the raw water source to produce humic acid concentrations ranging from 0 mg/L to 15 mg/L. The humic substances used in experiments were obtained in the form of sodium salt from Sigma-Aldrich (H16752). Polyaluminium chloride (PACl) coagulant doses (Holland Company. Adams, MA.) ranging from 0.53 mg/L as Al to 2.65 mg/L as Al were used to treat the synthetic raw water. The coagulant dosage and humic acid concentrations were regulated by adjusting the rotation speed of separate peristaltic pumps. The pH of the treated effluent was monitored in each experiment and was 7.5 $\pm$ 0.3. Influent turbidities of 50 NTU and 100 NTU were tested. Flocculation was accomplished by laminar flow through a coiled 9.52 mm (inner diameter) tube. The average velocity gradient in the flocculator, $\overline{G}$, was calculated by equation 1. The overall experimental flow rate was 6 mL/s and the radius of curvature of the coiled tubing (R_c) was 15cm.

$$\overline{G} = \overline{G_{Straight}} \sqrt{1 + 0.033 \left[log \left(\frac{4Q_{plant}}{\pi D \nu} \sqrt{\frac{D}{R_c}} \right) \right]^4} \quad (1)$$

Where $\overline{G_{Straight}}$ is fluid velocity gradient in a straight tube,

Q_{plant} is the experimental flow rate,

D is the inner diameter of the flocculator tube,

R_c is the diameter of curvature of the flocculator coils.

ν is the kinematic viscosity of fluid which is $1\times 10^{-6}\ \frac{m^2}{s}$ at 25 °C.

In laminar flow, $\overline{G}$ is related to the energy dissipation rate, ε, by Eq 2. The experimental $\overline{G}$ of 69.5 s^{-1} corresponds to ε of 4.83 mW/kg. The hydraulic residence time, θ, calculated by Eq 3, was 302 s.

$$\varepsilon = \nu \overline{G}^2 \quad (2)$$

$$\theta = \frac{\pi D^2 L}{4Q_{plant}} \quad (3)$$

where L is the length of the tube, and was 25.45m in the experiments.

A tube flocculator was used in this research because it can be idealized as a high-Péclet-number reactor much like a baffled hydraulic flocculator and also because the average velocity gradient in laminar tube flow is well defined (Weber-Shirk and Lion 2010). After continuous flow through the flocculator and a tube settler, the outflow

turbidity was recorded continuously for each experiment. The 1.37 m (4.5 ft) tube settler (whose inner diameter is 2.66 cm) has an entry port diameter of 0.95 cm (3/8 in) near the bottom and an exit port diameter of 0.635 cm (1/4 in) near the top, and the angle of inclination was 60 degrees. The capture velocity was controlled at 0.12 mm/s using a peristaltic pump.

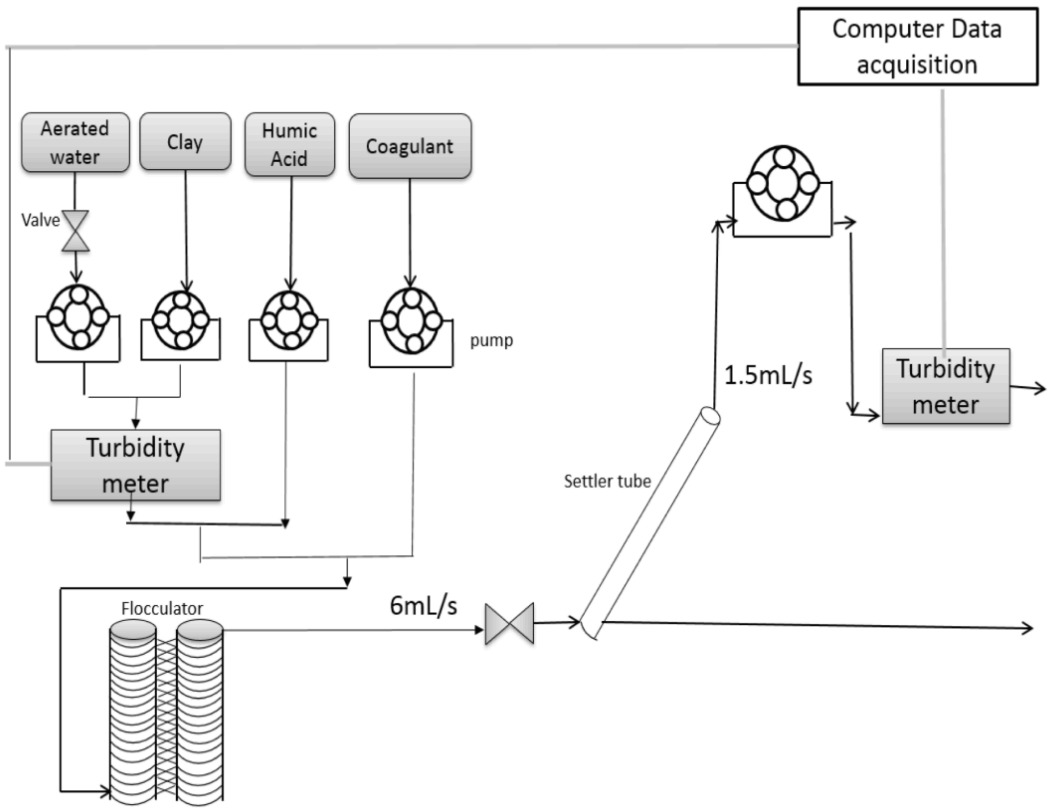

Figure 1: Experimental System Schematic

2.4 Model Formation

A flocculation model considering the effects of humic acid should predict the effective collisions between colloids for a given set of conditions. The dimensionless

term $\overline{G}\theta$ has been used as a measure of the collision potential provided by a flocculator that experiences laminar flow, where $\overline{G}$ is the fluid velocity gradient and is proportional to the rate of collisions, and θ is the hydraulic residence time or total time over which collisions occur (Camp 1955; Cleasby 1984) [Eq. 1]. It is well known that not all collisions between suspended particles result in aggregation, and attachment efficiency, α, has been used to denote the fraction of successful collisions (AWWA 1999). The primary particle volume fraction, ϕ, which represent the properties of the suspension, gives the fraction of the volume of the suspension occupied by the influent primary particles [Eq. 4].

$$\phi = \frac{C_{Influent}}{\rho_{Clay}} \tag{4}$$

Where ϕ is the primary particle volume fraction, $C_{Influent}$ is the influent clay concentration, and ρ_{Clay} is the density of clay particles.

In laminar-flow flocculators, the velocity of one floc relative to another scales with the average separation distance between flocs. The time between floc collisions is inversely proportional to ϕ and directly proportional to the velocity between flocs (or the separation distance or $\phi^{\frac{1}{3}}$). The result is that for laminar flow, the average time for primary particle collisions scales with $\phi^{\frac{2}{3}}$ (Weber-Shirk and Lion 2010).

A laminar-flow hydraulic flocculator model was developed and validated based on the above analysis (Swetland, et al, 2014) [Eq. 5]. The particle removal efficiency,

pC^* [Eq. 6] , is linearly proportional to the log of the effective collision potential $\log(\overline{G}\theta\alpha\phi^{\frac{2}{3}})$.

$$pC^* = \log\left(\overline{G}\theta\alpha\phi^{\frac{2}{3}}\right) + b \quad (5)$$

$$pC^* = -\log\left(\frac{Effluent\ turbidity}{inflow\ turbidity}\right) \quad (6)$$

Where pC^* quantifies particle removal; $\overline{G}$ and θ are as defined above; α is attachment efficiency; and b is a fitting parameter dependent on the capture velocity used for sedimentation.

Unfortunately, α is not directly measurable, thus a measurable variable, the fractional coverage of the colloid surface by coagulant ($\Gamma_{CoagtoClay}$) was used by Swetland, et al. (2014) as an alternative to estimate attachment efficiency based on the assumption that flocculation is mediated by adherent precipitated coagulant aggregates that bridge between colloids. The Swetland et al. (2014) was able to predict the results of independent experiments with no adjustable parameters in the absence of added NOM.

Experimental results obtained with added humic acid present are shown in Figure 2 along with predictions based on Swetland's model [Eq. 5]. Clearly, additional model terms are needed to account for the effects of humic acid.

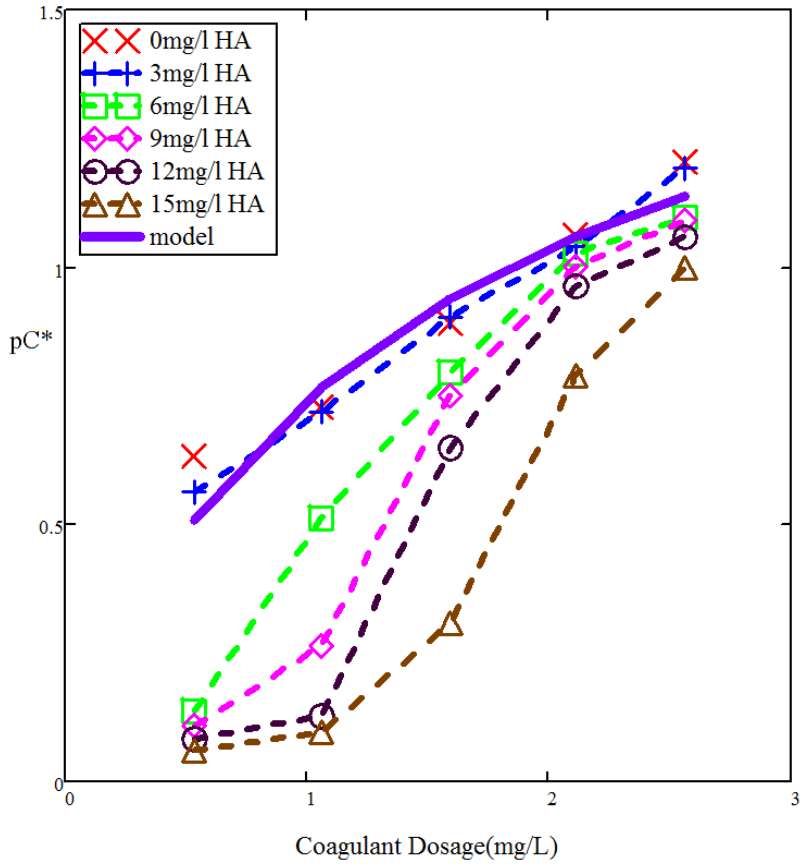

Figure 2: The original flocculation model fitting graph

It was evident that the attachment efficiency was adversely affected by the addition of humic acid. Approximately 20% of added DOC would be adsorbed by kaolinite at the experimental pH of 7.5 (Davis, 1982). Thus, most humic acid macromolecules were available to attach to the added coagulant nanoparticles. The following simplifying assumptions were made to account for the presence of humic acids: 1) humic acid macromolecules attach to coagulant nanoparticles to form nanoaggregates. 2) nanoaggregates attach to clay and to the reactor walls. 3) the surfaces of precipitated coagulant nanoparticles promote adhesion while the surfaces of bound humic acids prevent adhesion.

In this study, we modeled humic acid macromolecules and PACl nanoparticles as spheres. Based on size of coagulant nanoparticles and humic acid. N_{HA} and N_{PACI}, the number concentration of humic acid macromolecules and coagulant nanoparticles respectively, can be estimated by Eq. 7 and 8.

$$N_{HA} = \frac{C_{HA}}{\rho_{HA}\frac{\pi}{6}{d_{HA}}^3} \quad (7)$$

$$N_{PACI} = \frac{C_{PACI}}{\rho_{PACI}\frac{\pi}{6}{d_{PACI}}^3} \quad (8)$$

Where C_{PACI} is the dose of coagulant; C_{HA} is the concentration of humic acid; ρ_{PACI} is the density of the coagulant, $1138\ kg/m^3$ based on laboratory measurement; ρ_{HA} is the density of humic acid, $1780\ kg/m^3$ (Dinar, 2006); d_{HA} is the diameter of humic acid macromolecules; d_{PACI} is the diameter of coagulant nanoparticle, 90 nm (Garland 2015).

The model assumption was that humic acid macromolecules cannot adhere to a coagulant surface that is occupied by a humic acid macromolecule since humic acid macromolecules do not self-aggregate. Thus, humic acid macromolecules attach to an uncovered surface of coagulant and do not stack on top of one another. The available surface area of the PACl nanoparticle is modeled as the surface area of an equivalent sphere. The amount of that area that is occupied by an attached humic acid macromolecules is estimated as the projected area of an equivalent sphere. A new variable $\Gamma_{HAtoCoag}$ was created to be incorporated in the model to represent the

fraction of the PACl nanoparticle surface area that is covered by humic acid macromolecules [Eq. 9].

$$\Gamma_{HAtoCoag} = \frac{\frac{\pi}{4}{d_{HA}}^2}{\pi {d_{PACI}}^2} \frac{N_{HA}}{N_{PACI}} \quad (9)$$

The humic acid macromolecules attached to coagulant nanoparticles formed nanoaggregates. The nanoaggregates attach to clay particles. These first two steps in particle aggregation are assumed to be rapid because diffusion is an effective transport process for nanoparticles. The clay particles with attached nanoaggregates undergo collisions during the flocculation process and the aggregation process is governed by fluid shear. The success of a collision between clay particles is hypothesized to be dependent on the properties of the contact surfaces at the initial point of contact.

The 3 types of surfaces (PACl, humic acid, clay) have 6 (3!) potential interactions illustrated in Fig. 3.

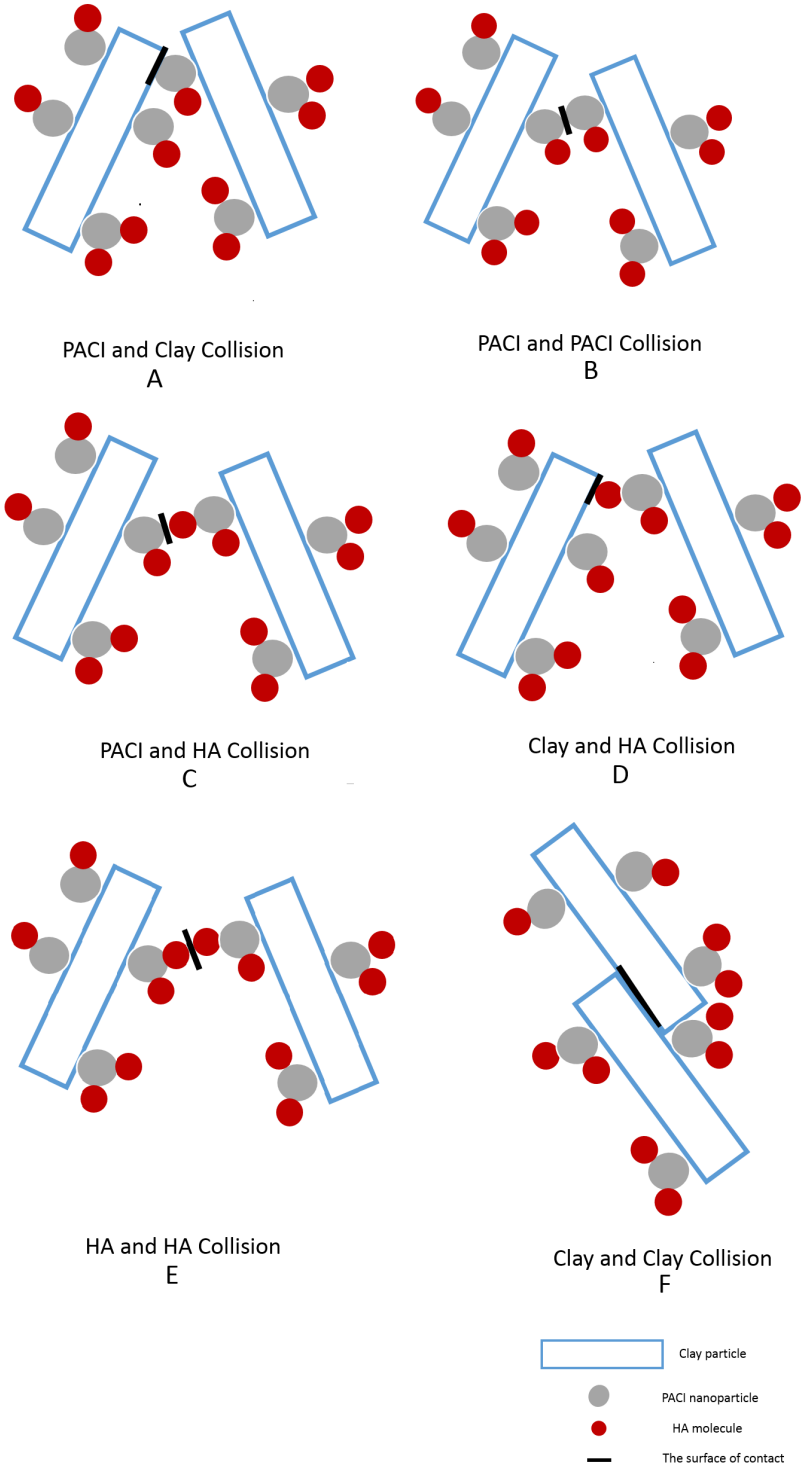

Figure 3: Collision between particles during flocculation

Of these interactions the only collisions that will result in attachment must involve at least one PACl nanoparticle surface (Figure 3 A, B, C). The attachment efficiency is hypothesized to be the sum of probability of these three types of collisions (Eq. 10).

$$\alpha = \alpha_{Clay-PACI} + \alpha_{PACI-PACI} + \alpha_{HA-PACI} \quad (10)$$

where the subscripts define the two surfaces that are interacting.

Based on the meanings of $\Gamma_{CoagtoClay}$ and $\Gamma_{HAtoCoag}$ described above, the fraction of clay surface is $1 - \Gamma_{CoagtoClay}$, the fraction of coagulant surface is $\Gamma_{CoagtoClay}(1 - \Gamma_{HAtoCoag})$, and the fraction of humic acid surface is $\Gamma_{CoagtoClay}\Gamma_{HAtoCoag}$.

The probability of a clay surface colliding with a PACl surface (Figure 3A) is equal to twice the probability that the first surface is clay and the second surface is the PACl surface of a PACl-HA nanoaggregates.

$$\alpha_{Clay-PACI} = 2(1 - \Gamma_{CoagtoClay})[\Gamma_{CoagtoClay}(1 - \Gamma_{HAtoCoag})] \quad (11)$$

The probability of a collision between two PACl surfaces of PACl-HA nanoaggregates (Figure 3B) is given by

$$\alpha_{PACl-PACI} = [\Gamma_{CoagtoClay}(1 - \Gamma_{HAtoCoag})]^2 \quad (12)$$

The probability of a collision between a PACl surface of a PACl-HA nanoaggregate and a HA surface of a PACl-HA nanoaggregate (Figure 3C) or vice versa is given by

$$\alpha_{PACl-HA} = 2[\Gamma_{CoagtoClay}(1 - \Gamma_{HAtoCoag})][\Gamma_{CoagtoClay}\Gamma_{HAtoCoag}] \quad (13)$$

The final model is modified from the Swetland et al. (2014) model by redefining the attachment efficiency using Eq.10 to account for the presence of humic acid.

The physical properties of humic acid vary from different sources. The diameter of humic acid macromolecules is estimated in range from 4 nm to 110 nm (Osterberg, 1993). Because of the variation of the size of the humic acid particles, we used the characteristic diameter of the humic acid macromolecules particles as a fitting parameter. Thus, there are two adjustable model parameters, b (equation 5) and d_{HA}. The model was validated by predicting results from independent data sets.

2.5 Results

The results from 60 experiments are shown in Table. 1 for an inflow turbidity of 50 NTU with PACl doses ranging from 0.53 to 2.65 mg/L and humic acid concentration ranging from 0 to 15 mg/L. A capture velocity of 0.12 mm/s was used in the experiments which is a conservatively designed lamellar settler capture velocity (Willis, 1978). Experiments were replicated for each combination of humic acid and PACl dose.

Table 1: Effluent turbidity results for experiments *conducted at 50 NTU.*

Turbidity (NTU) HA Concentration (mg/L)	Coagulant Dose (mg/L)	0.53	1.06	1.59	2.11	2.65
0	replicate 1	11.61	8.51	5.73	4.34	3.12
	replicate 2	12.44	8.13	5.86	4.25	3.24
3	replicate 1	14.00	9.16	6.25	4.58	3.21
	replicate 2	14.65	8.75	5.97	4.48	3.25
6	replicate 1	36.56	15.35	8.05	4.70	4.02
	replicate 2	37.41	14.65	7.69	4.63	3.93
9	replicate 1	38.90	27.23	8.91	4.98	4.07
	replicate 2	39.63	26.98	8.51	4.91	4.04
12	replicate 1	41.21	37.24	11.27	5.46	4.39
	replicate 2	40.83	37.50	11.32	5.58	4.29
15	replicate 1	43.45	40.27	24.60	8.17	5.02
	replicate 2	42.95	40.18	25.18	7.98	5.04

The data shows that increased coagulant dose is positively correlated with turbidity removal. The effluent turbidity was greatly increased by the presence of humic acid. In all cases, increasing the coagulant dosage resulted in decreasing settled water turbidity. Transforming the residual turbidity by Eq. 6. the observations for 50 NTU raw water are shown in Fig 4.

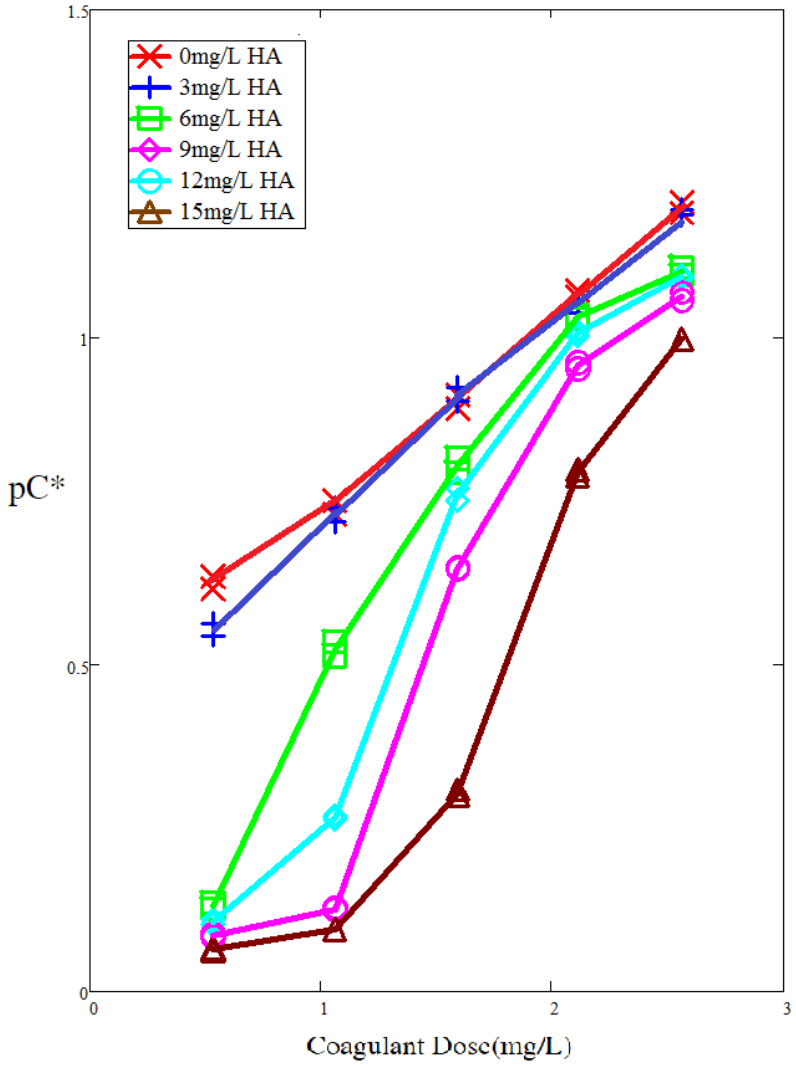

Figure 4: pC as a function of coagulant dose for 50 NTU inflow turbidity*

Applying the model to the raw data, and adjusting the two fitting parameters, b and d_{HA} to minimize the sum squared error gave b = 0.13 and $d_{HA} = 36\ nm$ (data points with pC* less than 0.5 were not considered for purposes of model fitting), with $R^2 = 0.92$. Figure 5 shows the fit of the model to the observations for the 50 NTU experiments.

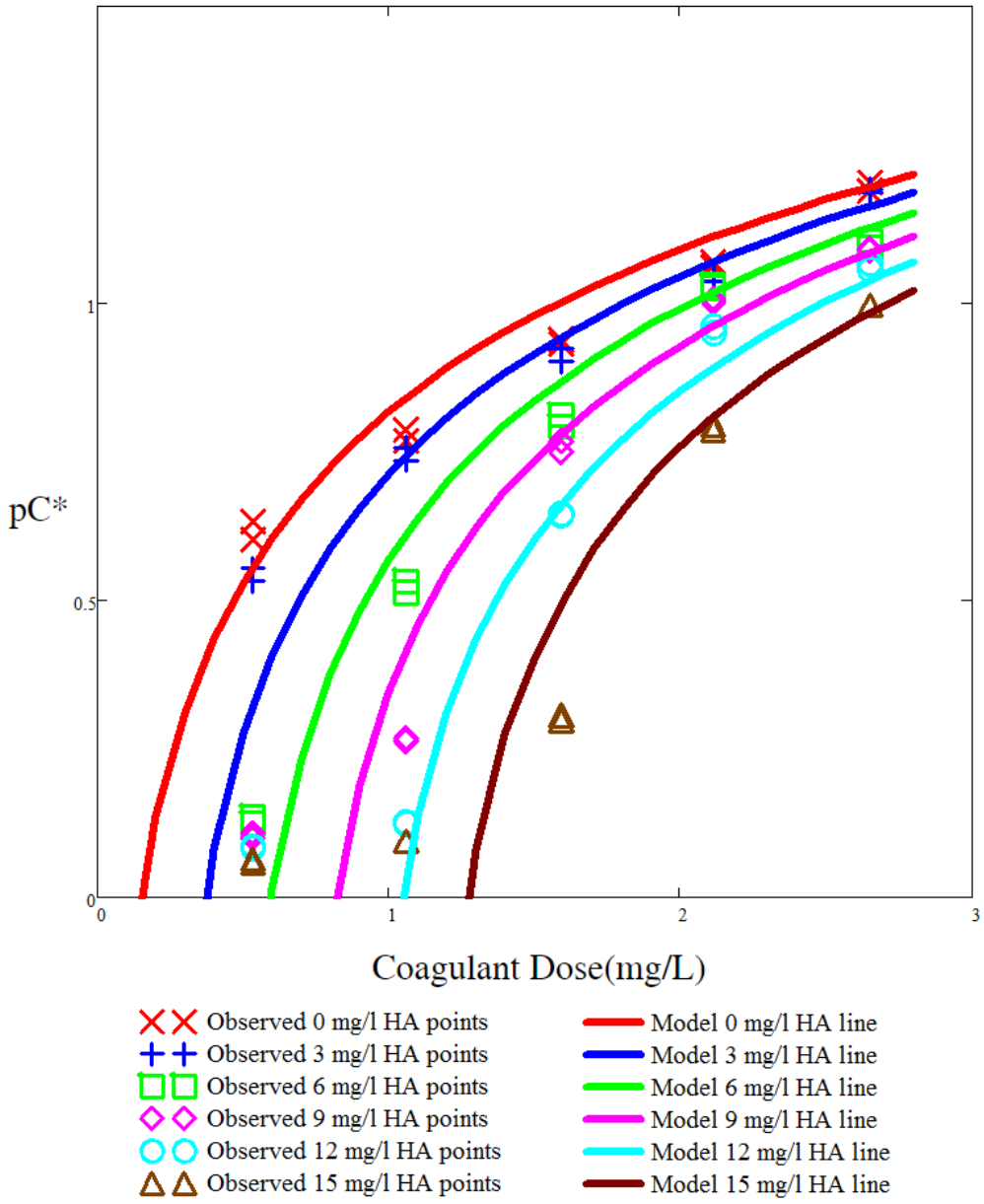

Figure 5: Model fit for pC as function of coagulant dose for 50 NTU raw water turbidity.*

When the coagulant dose in Fig. 5 was replaced with $\overline{G}\theta\alpha\phi^{\frac{2}{3}}$, the data collapse to a much narrower band implying the composite parameter, $\overline{G}\theta\alpha\phi^{\frac{2}{3}}$, captures a large fraction of the trends present in the data (Fig 6).

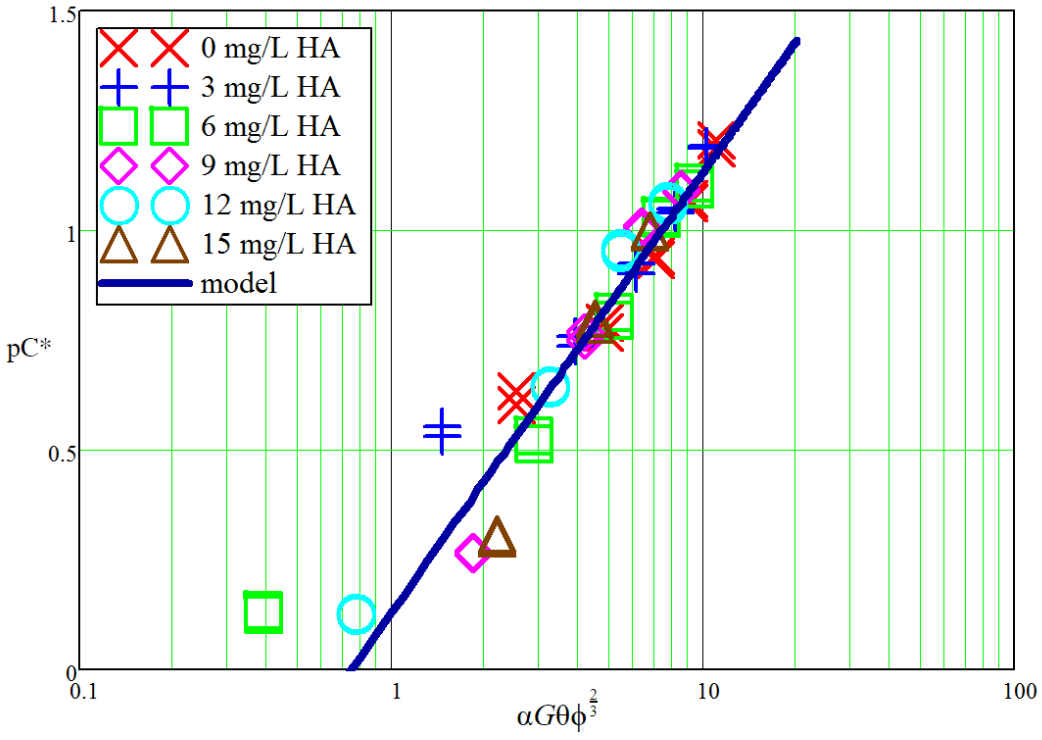

Figure 6: Model fit for pC as function of effective collision potential*

With the given fitting parameter $d_{HA} = 36\ nm$ for influent turbidity 50 NTU dataset, the new variable $\Gamma_{HAtoCoag}$ changes as shown in figure 7. The model predicts complete coverage of the PACl nanoparticles by humic acid for low PACl concentrations and that correlates with very low observed turbidity removal efficiency. The relationships between the three terms included in attachment efficiency, coagulant dose and humic concentration are shown in the figure 8. The $\alpha_{Clay-PACl}$ is always

dominant for the experimental conditions in this dataset, and $\alpha_{PACI-HA}$ becomes significant when the coagulant dose and humic acid concentration are high.

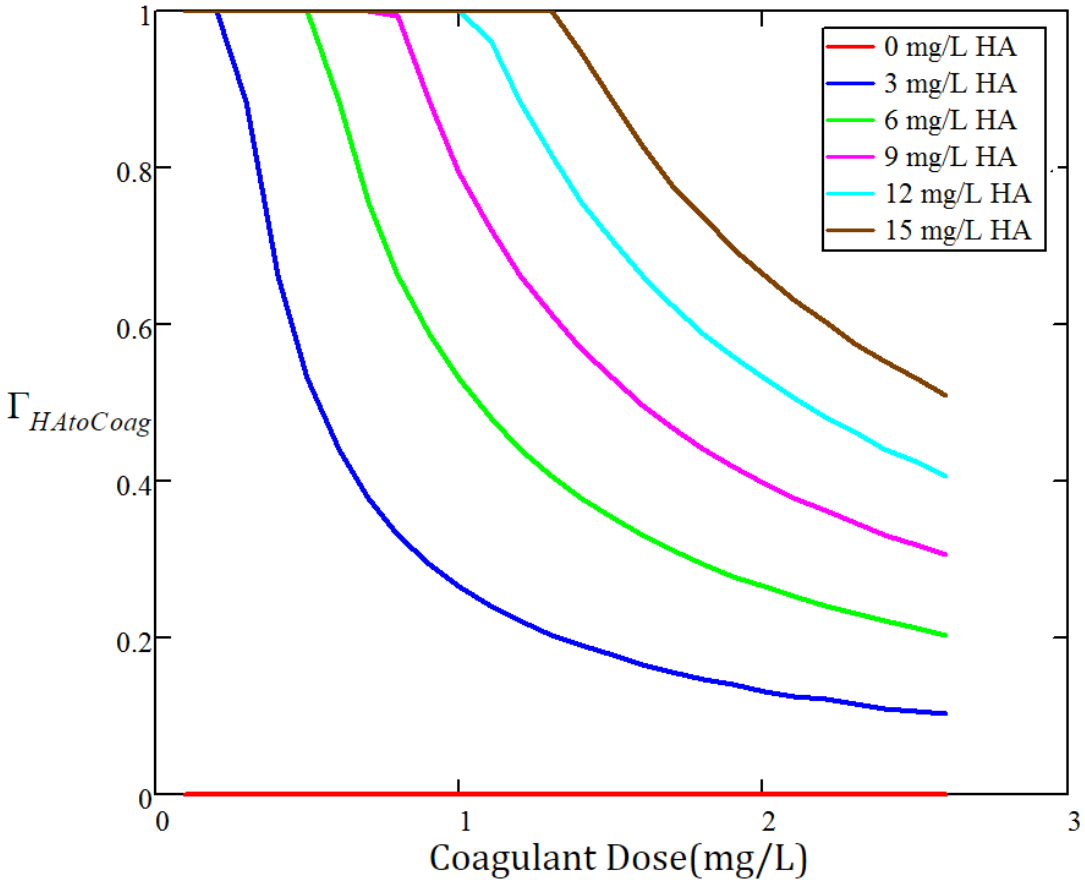

Figure 7: Coverage of coagulant surface by humic acid as a function of coagulant Dose

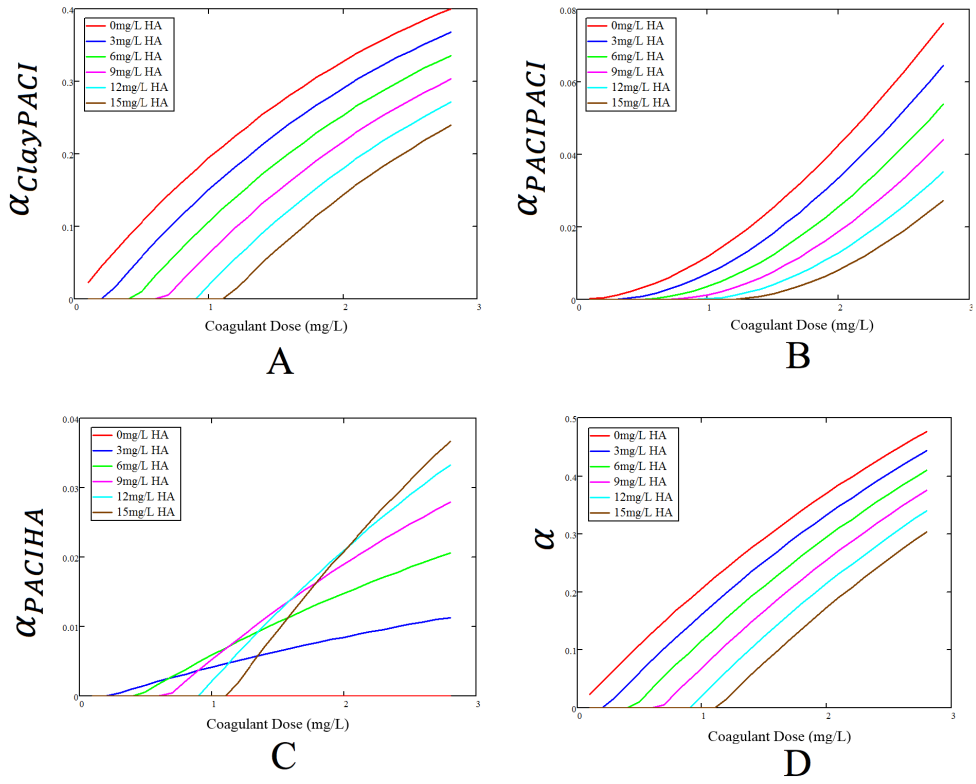

A. Attachment efficiency between clay particle surface and a PACl surface of a PACl-HA nanoaggregate as the function of coagulant dose
B. Attachment efficiency between two PACl surface of a PACl-HA nanoaggregate as the function of coagulant dose
C. Attachment efficiency between a PACl surface of a PACl-HA nanoaggregate and a HA surface of a PACl-HA nanoaggregate as the function of coagulant dose
D. Attachment efficiency as the function of coagulant dose

Figure 8: Attachment efficiencies as a function of coagulant dose

The model was validated by using it to predict turbidity removal efficiency for different experimental conditions. The predicted pC* and the measured pC* are compared in fig. 9 for an additional 60 experiments with inflow turbidity of 100 NTU, PACl doses ranging from 0.53 to 2.65 mg/L and humic acid concentration

ranging from 0 to 15 mg/L. The resulting $R^2 = 0.87$ for agreement of the model predictions with the observations.

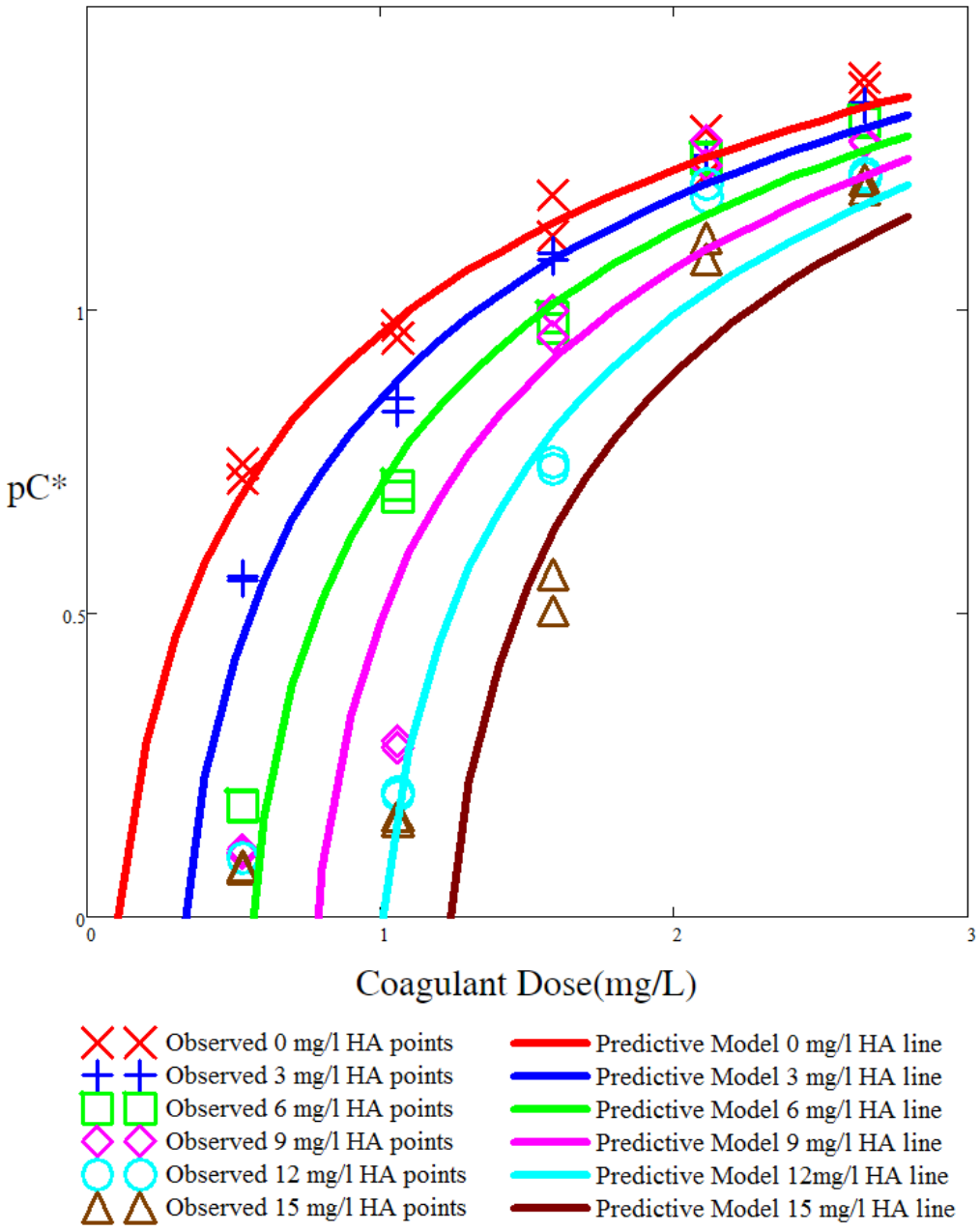

Figure 9: Comparison graph between predicted data and observed data for 100 NTU influent turbidity

In summary, the laminar flow hydraulic flocculation model of Swetland et al. (2014) was modified to incorporating the effects of humic acid with the addition of a single fitting parameter, the characteristic dimension of the humic acid macromolecules. The required coagulant dose can be predicted based on the flocculator parameters, humic acid characteristic size and concentration, and influent turbidity. The addition of humic acid to the flocculation model increases the model applicability since natural organic matter is found in all surface, ground and soil waters and influences the coagulant dose needed for effective turbidity removal.

For the range of experimental conditions considered in the research, the observed influence of humic acid on flocculation performance could be explained by the fractional coverage of the coagulant surface by humic acid, which, in turn, affected the fractional coverage of the colloid surface by coagulant. It is noteworthy that under the experimental conditions, the predictive success of model was achieved without incorporating the charge of colloids, coagulant, and humic acids. The reader is cautioned that the observations and predictions were obtained with one test colloid, one coagulant, and one humic acid, in the narrow pH range where coagulant precipitation is very favorable, in the mixed electrolyte represented by Cornell tap water. While the experimental pH favored PACl precipitation, pH dependent PACl solubility is accounted for in the model.

While the pH dependence of coagulant solubility is a component of the model, the solubility of humic acid also is highly pH dependent, and additional experimental results are needed to test the applicability of the model approach as a function of

varying pH. The experimental conditions were designed to keep the pH relatively constant and the pH change in the experiments was small (7.0-7.5).

The model considered the flocculation in the presence of humic acid as a two step process. Firstly, humic acid macromolecules attached to precipitated coagulant nanoparticles. Then, the partially coated coagulant nanoaggregates could bind to clay and reactor wall surfaces. Humic acid and coagulant nanoparticles were treated as spheres when estimating the attachment efficiency based on surface coverage and probability. The estimated diameter of precipitated PACl nanoparticles was experimentally measured to be 90 nm (Garland, 2016), and a humic acid macromolecule diameter of 36 nm best fit the observations. Wall loss of coagulant precipitates with humic acid nanoaggregates was considered while direct wall loss of humic acid macromolecules was not considered.

The additional parameter, d_{HA} , has a physical meaning and the model fits are well correlated to the observations. The predictive capability of the model was verified by predicting results under different experimental conditions with no additional adjustable parameters.

The flocculation model without the effects of humic acid shows that pC* is directly proportional to the log of the effective collision potential $\log(\alpha G\theta\phi^{\frac{2}{3}})$ and this relationship is still present in the model with a modified attachment efficiency, α, based on clay surface coverage by coagulant nanoparticles as adjusted for the presence of humic acids.

Under experimental conditions, the modified flocculation model provides the fundamental basis for the relationship between coagulant dose, synthetic raw water clay and humic acid concentrations. Extension to natural waters will undoubtedly require additional research.

The six terms in the flocculation model equation set the interactions between raw water properties (ϕ) and colloid surface area (which contributes to $\alpha_{Coag-Clay}$), coagulant precipitate size and dose (which contribute to $\alpha_{Coag-Clay}$ and $\alpha_{HA-Coag}$), humic acid molecule size and concentration (which contribute to $\Gamma_{\mathrm{HA-Coag}}$), flocculator design ($G\theta$), and sedimentation tank design ($V_{Capture}$). In a water treatment plant operating at constant flow rate, the flocculator and sedimentation tank parameters are constant. An increase in concentration of humic acid causes an increase in $\Gamma_{HA-Coag}$, which decreases pC*.

2.6 Conclusions and Recommends

The development of a predictive model for laminar flow hydraulic flocculation of water containing clay and humic acid is described. The study results increase the flexibility and generality of the flocculation model and the modified model provides insight into the mechanism by which humic acid causes a decrease in performance of coupled flocculation-sedimentation processes.

The model was able to predict results for a different raw water turbidity with no additional adjustable parameters. Further tests should be done to fully validate the laminar-flow model including consideration of different experimental surrogates for

NOM, different colloidal surfaces, alternative coagulants and varying solution compositions including pH.

CHAPTER 3: EFFECTS OF HUMIC ACID ON FLOCCULATION PARTICLE SIZE DISTRIBUTIONS

3.1 Image Analysis

In order to obtain data for floc size, an image analysis system was incorporated into the experimental apparatus to collect images for different experimental conditions [Fig. 10].

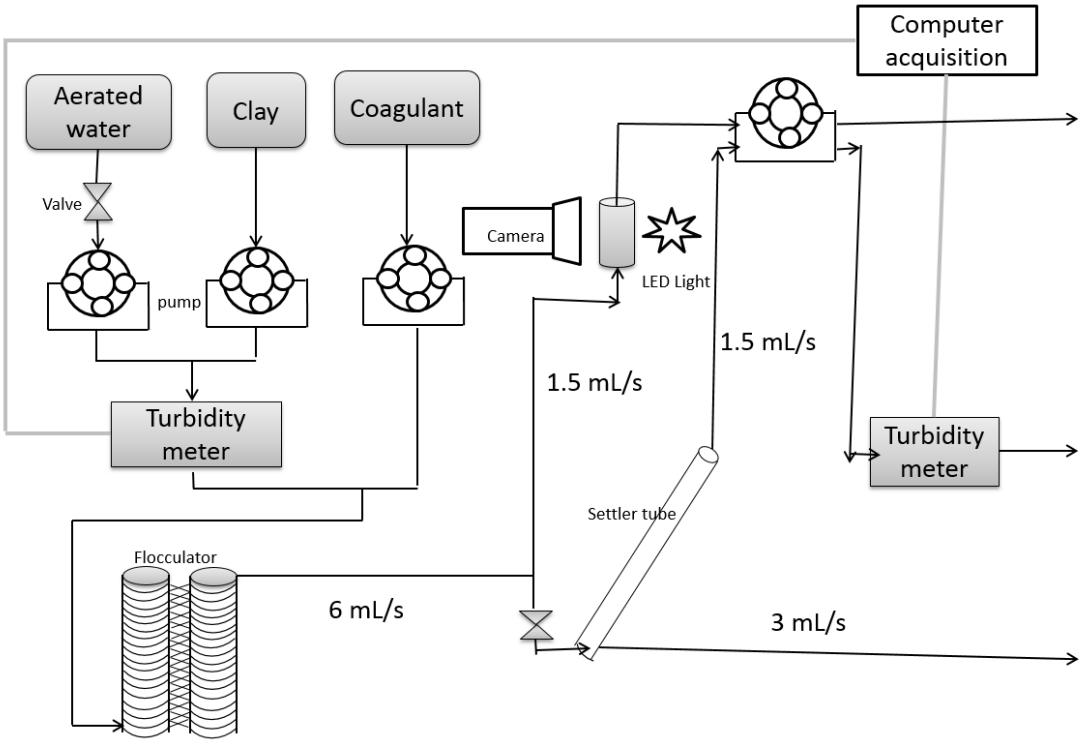

Figure 10: Experimental System Schematic with Image Analysis System

The camera system (see Fig 12) consisted of an LED light source and a BFLY-PGE-12A2M-CS 1/3" Blackfly® PoE GigE Monochrome Camera, with image

analysis using LabVIEW software. The camera was a 1280 × 960 pixels progressive scan, monochrome 1/3" CCD fitted with 5X compact adjustable objective lens with a numerical aperture of 13.7mm. The limitation of the image system was that, at low magnification (Fig 11), there are too many flocs in the field of view and flocs overlap. This creates inaccuracy in the identification of individual particles. Alternatively, at high magnification (Fig 11), the field view can become too small to contain large flocs and fully imaged flocs rarely occur in the field of view. As a result, it becomes difficult to collect data. The reasons for selection of a 5X compact adjustable objective lens were an experimental focus of small particles that will contribute to effluent turbidity.

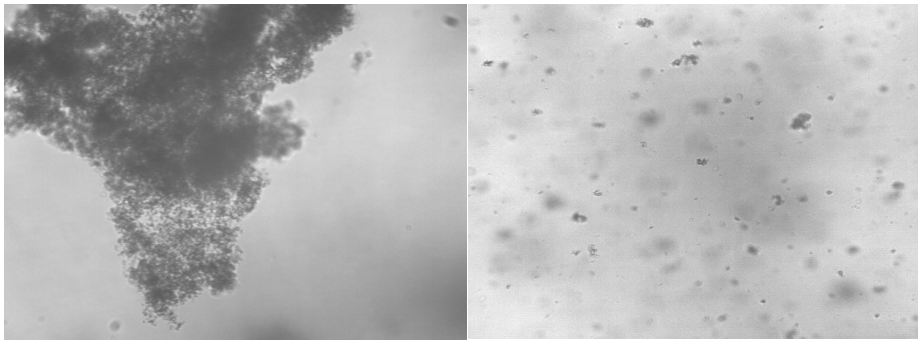

Figure 11: High magnification (Left) and Low magnification (Right)

The camera can capture continuous images at up to 52 frames per second or single images by external trigger or via software control.

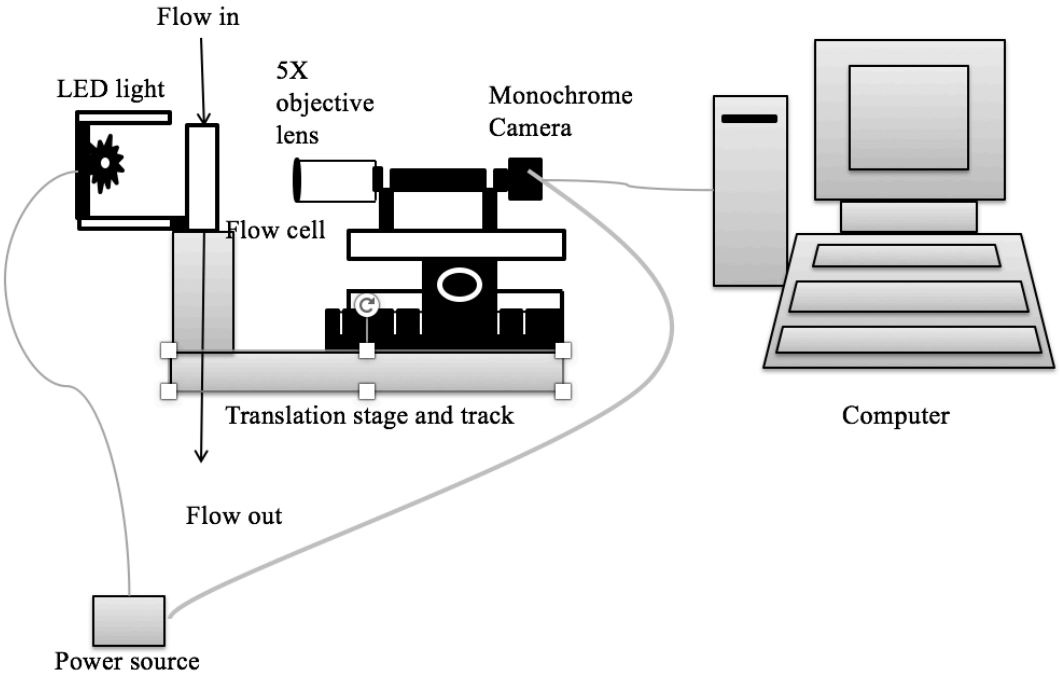

Figure 12: Imaging system consisting of LED light, CCD camera attached to a computer and the suspended sample in a flow cell.

The field of view in the image system is 0.96 mm (horizontal) × 0.72 mm (vertical) and the resulting pixel size is 0.74 μm based on the magnification and lens. The depth of the field of view was estimated as 0.98 mm based on the experiments (Casey Garland personal communication).

For the image analysis system in experiments, shutter time was in the range of 0.019 ms to 1.226 s, and particles in the flow cell could not move more than 1 pixel within the shutter time. The flow rate through image analysis system can be calculated by equation (14).

$$v_{flow} = \frac{D}{T} \tag{14}$$

Where, v_{flow} is the flow velocity through the image analysis system.

D is 1 pixel which equals to 0.74 μm

T is camera shutter time.

Also, the flow rate should be fast enough to guarantee that there no collisions occur in the flow cell. The apparatus system in the experiment tried to use one pump to control the capture velocity of tube settler and the flow rate through the floc cell, and the selected flow rate $1.5\,\frac{mL}{s}$ was selected because the rate was need for capture velocity and this flow rate is also within the reasonable range to take photos with negligible blurring.

The image analysis script used in the experiment accomplished four functions: (1) reduction of image noise, (2) identification of particles from background, (3) removal of particles that were out of focus or that had portions beyond the image border, (4) calculation and recording of particle sizes. The image processing functions prepackaged in LabVIEW are capable of identifying and measuring particles. These functions include filters, threshold, basic or advanced morphology and particle analysis ("Image analysis and processing," 2008). Sun (2015) improved the analysis system by removing out-of-focus particles. The procedure to analyze flocs size is shown in figure 13.

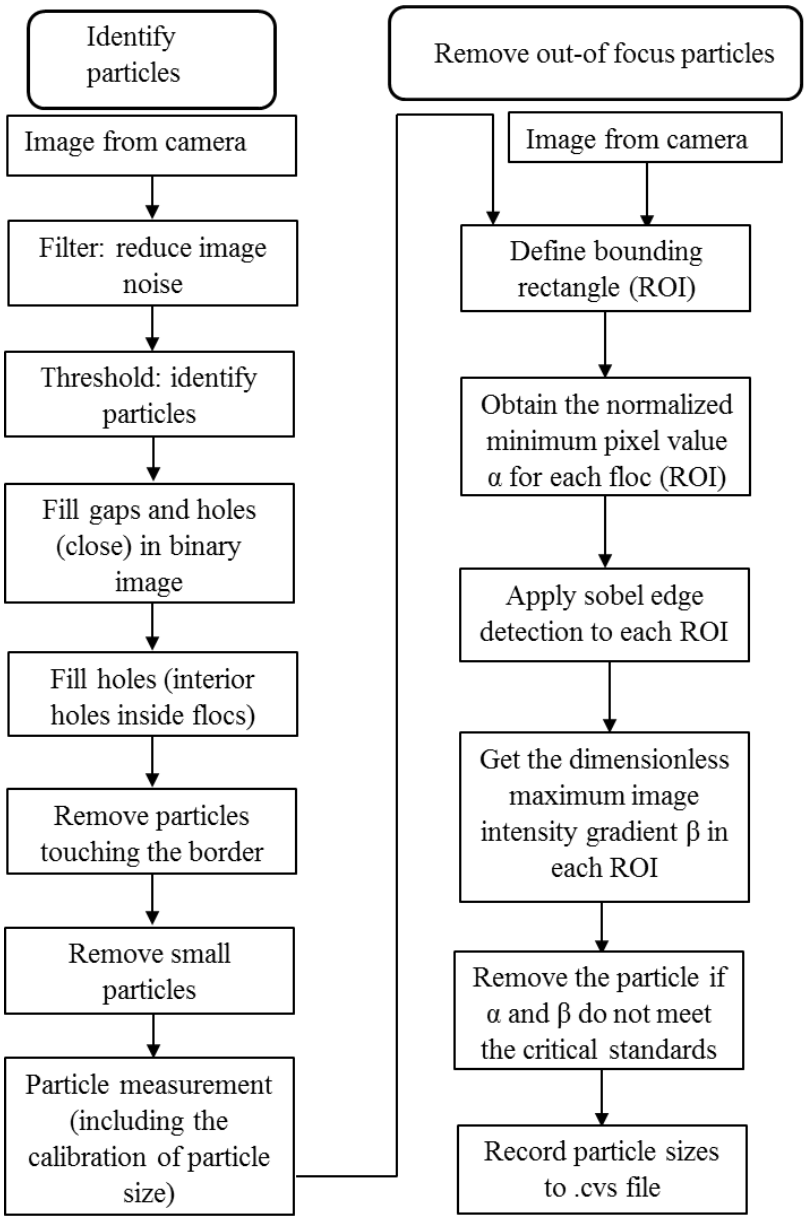

Figure 13: Flowchart of image analysis procedure (Sun, 2015).

Particle size distribution is a major parameter used to determine the effectiveness of flocculation. Flocculated particle suspensions are often quite heterodisperse and are characterized by broad and nearly continuous particle size distributions (PSDs) (Nason, 2006). Within the limitations of the experimental image system, large particles (>300 μm) were seldom captured, while the smaller particles have higher possibility to be

captured. Moreover, some light is adsorbed by suspension when the humic acid concentration is high, which results in failure of floc identification. Thus it was difficult to create a full PSD in the study.

For each experiments, the volume of water monitored is be calculated from Eq. 15.

$$V_{monitored} = N_{\ image} \times H_{FOV} \times V_{FOV} \times D_{FOV} \quad (15)$$

where $V_{monitored}$ is the volume of water monitored for each experiment; N_{image} is the number of images collected, H_{FOV} , V_{FOV}, and D_{FOV} are the length, height and depth of field of view.

Particle frequency is obtained from Eq. 16.

$$Frequency = \frac{N_{particle}}{V_{monitored}} \quad (16)$$

Where $Frequency$ means the number of particles per sample volume in a certain size range; $V_{monitored}$ is the the volume of water monitored for each experiment and $N_{particle}$ is the number of identified particles from the collected images.

3.2 Results

Particle size distribution (PSD) frequencies for the experiments with inflow turbidity 50 NTU and varying coagulant doses for humic acid concentrations of 0 and 3 mg/L are shown below (Fig 14):

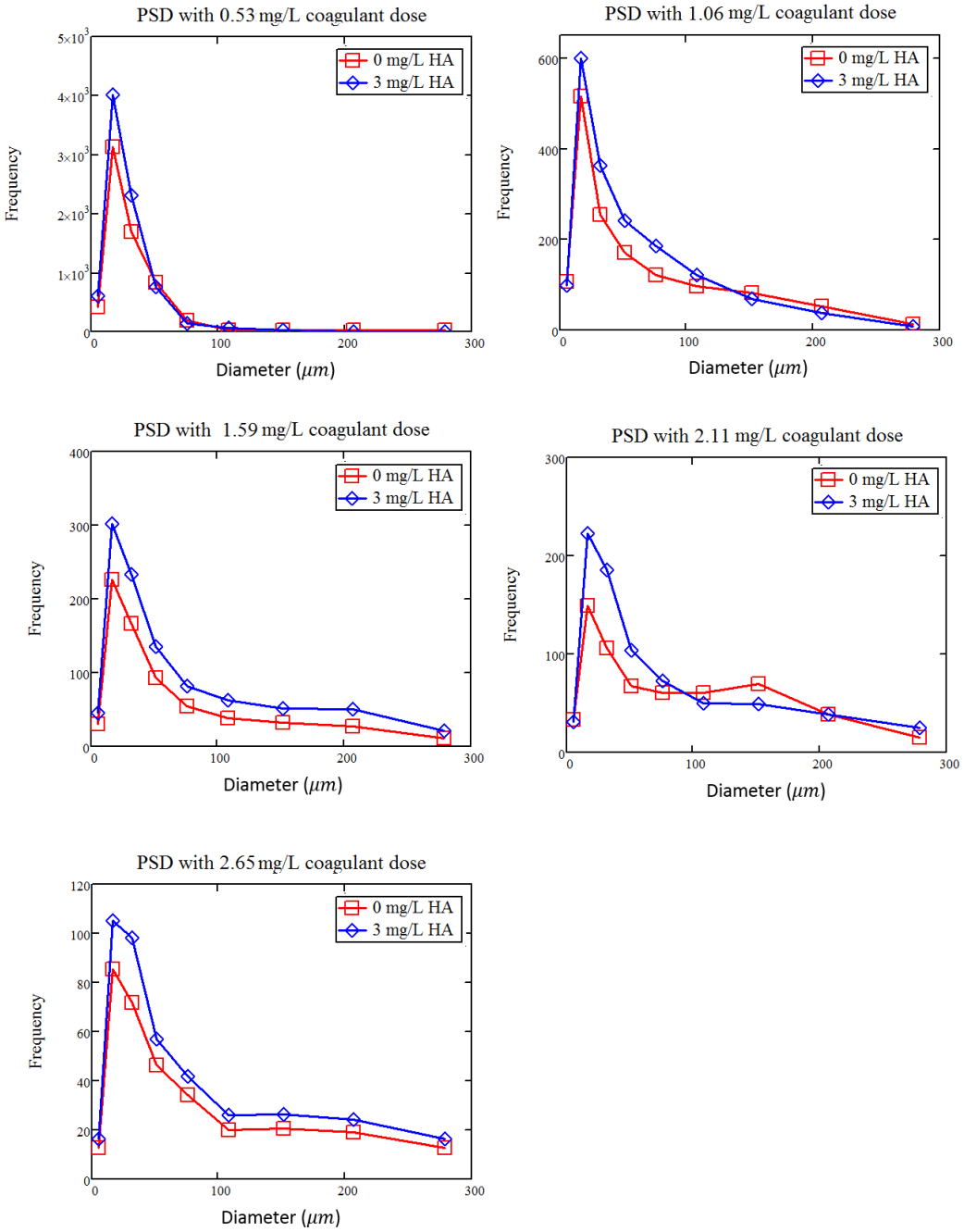

Figure 14: Comparison graphs for particle frequency distribution between experimental condition with 0 mg/L HA and 3 mg/L HA

The frequency of smaller particles after flocculation was increased when humic acid is present in the system. NOM could complex with the PACI to create PACI organic precipitates, resulting in a greater frequency concentration of small particles

(Snodgrass et al. 1984; Herrboldt 2016). The conclusion is also consistent with the model research in the chapter 2 that humic acid molecules would coat the coagulant nanoparticles and decrease the attachment efficiency of the collisions.

Image analysis was not possible for experiments with high humic acid concentrations and high coagulant doses. Humic acid at high concentrations strongly absorbs light and the images collected had poor contrast for identification of particles.

Results for different coagulant doses are shown in Figure. 15. Data for low coagulant doses (0.53 mg/L and 1.06 mg/L) were not successfully collected since the images collected become too dark to be identified flocs with high humic acid concentration and low coagulant dose. The raw data indicate that the number of small particles (< 50 µm) increased with increasing concentration of humic acid, and the increase in more obvious with low coagulant doses.

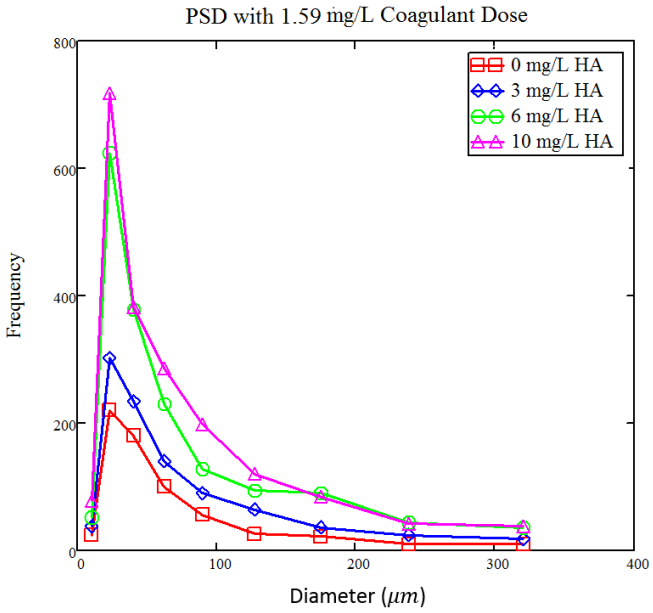

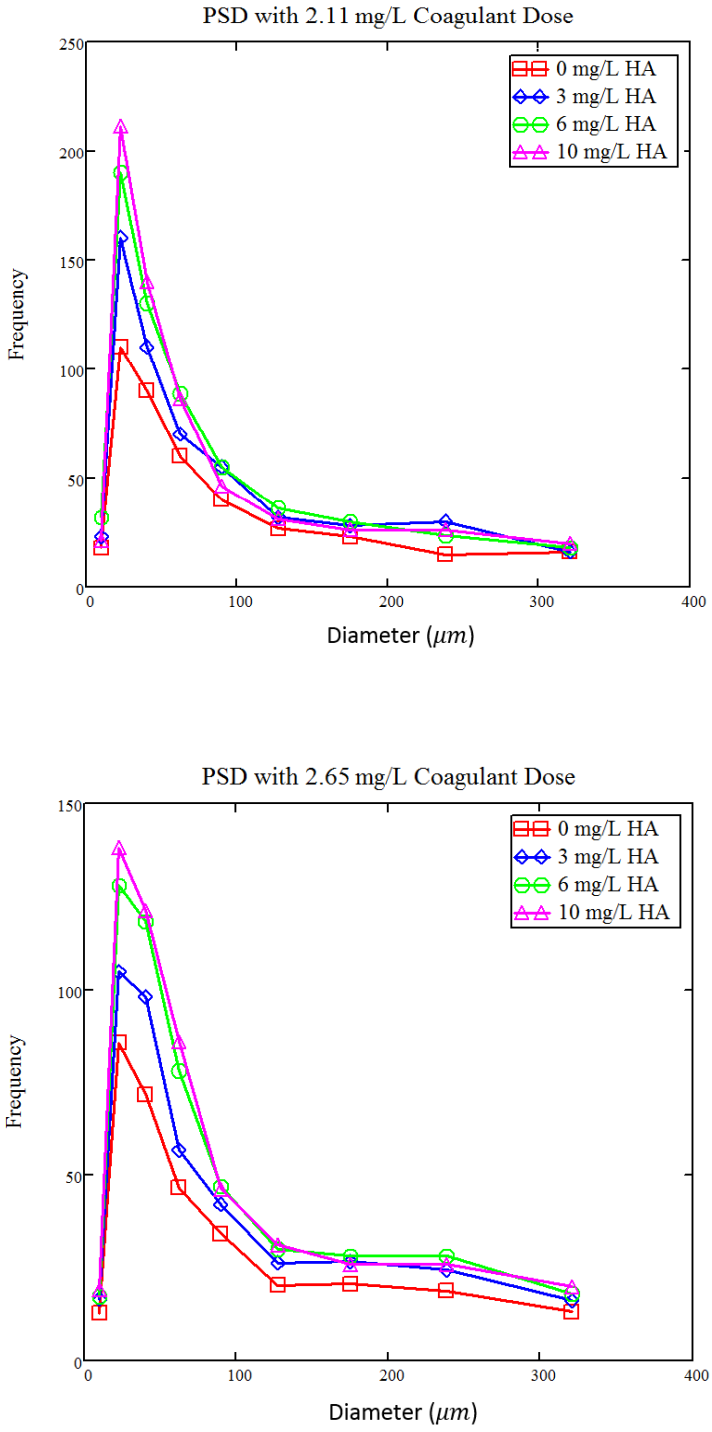

Figure 15: Comparison graphs for particle frequency distribution with variations of HA and coagulant doses

3.3 Conclusions

Coagulation has the potential to enable water systems to meet treatment goals for NOM. However, one drawback is that humic acid may affect the settling and filtration characteristics of the precipitated solids by changing the particle size distribution of these solids. This work was aimed at developing an understanding of how humic acid changes particle sizes in the system. The particle diameter associated with the peak of the frequency distribution is shift toward a lower value, which indicates large particle formation and aggregation is inhibited by the present of humic acid.

The floc size identification was inaccurate when too many flocs passed through the flow cell concurrently. Moreover, the light source was not strong enough to permit photos for flocs when the humic acid concentration was high and the coagulant dose was insufficient.

Future work is needed to improve the imaging technology and explore the effects of humic acid on the size distribution of particles after hydraulic flocculation.

CHAPTER 4: CONCLUSIONS AND RECOMMANDATIONS

The thesis presents the development of predictive model for settled effluent turbidity subsequent to hydraulic flocculation under laminar flow with consideration of the effects of the humic acid by redefining the attachment efficiency in Swetland et al's (2014) model. The revised model was developed based on the observation of residual turbidity for a range of PACl coagulant dose (0.53 – 2.65 mg/L) and humic acids concentration (0 – 15 mg/L) with inflow turbidity of 50 NTU. The term $\Gamma_{HAtoCoag}$ was incorporated into the flocculation model to account for the effects of humic acid. One adjustable parameter d_{HA} is employed to describe the properties of the humic acid in the raw water. In the model, humic acid macromolecules were treated as spheres. The modified model was validated with independent experiments, and the modified parameter $\alpha G\theta\phi^{\frac{2}{3}}$ was able to predict results with no additional adjustable parameters. This study results increase the flexibility and generality of the flocculation model and the modified model provides improved guidelines for flocculator design and operation.

Future work is needed to test flocculator performance over a broad range of values of the composite parameter ($\alpha G\theta\phi^{\frac{2}{3}}$), with individual components of the composite parameter being varied. A battery of experiments in which all of these variables have a wide range of values will provide a dataset that should ideally collapse to one line when plotted against the composite parameter. If this is not the case, further

refinement will need to be made to the composite parameter. The goal for this model is to accurately represent the dominant mechanisms of flocculation using as inputs the characteristics of the flocculator and sedimentation tank as well as the influent water characteristics to predict the turbidity leaving the sedimentation tank. Future research can consider the effect of pH and other types of NOM such as fulvic acid.

In this study, the influence of humic acid on floc size distributions was also described. Results in the study showed that large floc formation is inhibited by the present of humic acid. Further investigation into the influence of humic acid on floc size is warranted and should focus on coagulant dosages that are sufficient to ensure that the humic acid is attached to the coagulant nanoparticles.

APPENDIX

1. Flow rate, coagulant dose and influent turbidity

A flow rate of 6 mL/s through the apparatus met the minimum 1.67 mL/s requirement for the turbidity meter and also met the requirement to guarantee the target G is about $70s^{-1}$. There are two 100 rmp pumps to control clay addition and coagulant dose separately, and the tubes used for the two pump are "yellow-blue" (D = 1.52 mm) and "orange-yellow" (D = 0.51 mm) respectively. PACl coagulant doses (Holland Company. Adams, MA.) ranging from 0.53 to 2.65 mg/L as Al were mixed into the raw water. The flow rate needed for the coagulant solution was calculated by the law of conservation of mass.

$$Q_{Al} = Q_{plant} \times \frac{C_{plant}}{C_{Al}} \tag{17}$$

Where, Q_{Al} is the flow rate of coagulant solution,

Q_{plant} is the flow rate through the flocculator,

C_{plant} is the Al dose within the flocculator,

C_{Al} is the Al concentration of coagulant stock.

Equation (18) was used to calculate the concentration of clay added to water, the value of 1.73$\frac{mg}{L \cdot NTU}$ was measured in the lab by Casey Garland (personal communication, June 13, 2015).

$$C_{clay} = 1.73 \frac{mg}{L \cdot NTU} \cdot Target\ NTU \quad (18)$$

Where, $Target\ NTU$ is 50 NTU in the experimental condition.

2. Tube Settler

The 1.37 m (4.5 ft) tube settler (whose inner diameter is 1.049 inch) has an entry port diameter of 0.95 cm (3/8 in) near the bottom and an exit port diameter of 0.635 cm (1/4 in) near the top, as is shown in figure 16.

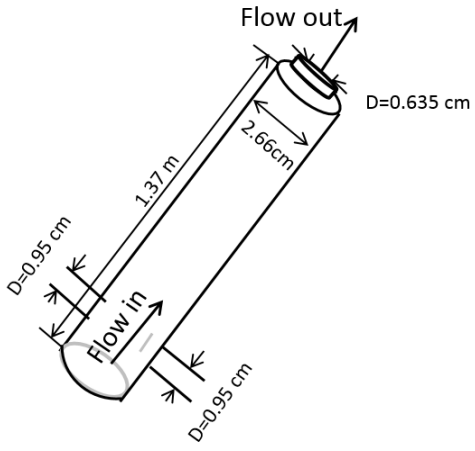

Figure 16: Tube settler

The tube settler capture velocity was determined by equation 19.

$$v_{up} = v_{tube\ settler} \cdot \sin\theta \tag{19}$$

$$v_{capture} = \frac{v_{up} \cdot d}{L_{tube\ settler} \cdot \cos\theta \cdot \sin\theta + d} \tag{20}$$

where v_{up} is the vertical component of the velocity in the setting tube ($v_{tube\ settler}$) and $v_{capture}$ is the capture velocity. θ is the angle of the tube settler (60 degrees) and d is the inner diameter of the tube settler. $L_{tube\ settler}$ is the length of tube settler. Sedimentation occurred in a tube settler with a capture velocity (also referred to as a critical velocity) of 0.12 mm/s. $v_{tube\ settler}$ was obtained by combining (18) and (19).

$v_{tube\ settler}$ is $3.224\times10^{-3}\,\frac{m}{s}$, and the Q in tube settler should be $1.5\,\frac{mL}{s}$

REFERENCES

American Water Works Association (AWWA). (1999). Water quality and treatment, 5th Ed., McGraw-Hill, Denver, CO.

AguaClara. 2017. “AguaClara Plants.” <http://aguaclara.cee.cornell.edu/about/projectmap/> (Jul. 7, 2017).

Amin, Mohammad Mehdi, et al. "Feasibility of humic substances removal by enhanced coagulation process in surface water." International Journal of Environmental Health Engineering 1.1 (2012): 29.

Bolton Point Water System. (2012). “Drinking water quality report Southern Cayuga Lake intermunicipal water commission.” Technical Rep., Bolton Point Municipal Water System, Ithaca, NY.

Garland, C. (2015). Size Measurement of PACl Precipitate Particles.

Camp, T. R. (1955). “Flocculation and flocculation basins.” ASCE Trans., 120, 1–16.

Cleasby, J. (1984). “Is velocity gradient a valid turbulent flocculation parameter?” J. Environ. Eng., 10.1061/(ASCE)0733-9372(1984) 110:5(875), 875–897.

Chow, Christopher WK, et al. "Assessing natural organic matter treatability using high performance size exclusion chromatography." Environmental science & technology 42.17 (2008): 6683-6689.

Dinar, E., T. F. Mentel, and Y. Rudich. "The density of humic acids and humic like substances (HULIS) from fresh and aged wood burning and pollution aerosol particles." Atmospheric Chemistry and Physics 6.12 (2006): 5213-5224.

Davis, James A. "Adsorption of natural dissolved organic matter at the oxide/water interface." Geochimica et Cosmochimica Acta 46.11 (1982): 2381-2393.

Evans, C. D., D. T. Monteith, and D. M. Cooper. "Long-term increases in surface water dissolved organic carbon: observations, possible causes and environmental impacts." Environmental pollution 137.1 (2005): 55-71.

Gregor, J. E., C. J. Nokes, and E. Fenton. "Optimising natural organic matter removal from low turbidity waters by controlled pH adjustment of aluminium coagulation." Water Research 31.12 (1997): 2949-2958.

Herrboldt, Jonathan Philip. Fluoride, natural organic matter, and particles: the effect of ligand competition on the size distribution of aluminum precipitates in flocculation. Diss. 2016.

Hu, Chun, et al. "Visible-light-induced photocatalytic degradation of azodyes in aqueous AgI/TiO2 dispersion." Environmental science & technology 40.24 (2006): 7903-7907.

Hua, Guanghui, and David A. Reckhow. "Relationship between brominated THMs, HAAs, and total organic bromine during drinking water chlorination." 2008. 109-123.

Matilainen, Anu, Mikko Vepsäläinen, and Mika Sillanpää. "Natural organic matter removal by coagulation during drinking water treatment: a review." Advances in colloid and interface science 159.2 (2010): 189-197.

Ives, K. J. (1968). “Theory of operation of sludge blanket clarifiers.” Proc. Inst. Civil Eng., 39(2), 243–260.

Jarvis, Peter, et al. "A review of floc strength and breakage." Water research 39.14 (2005): 3121-3137.

KA Swetland, ML Weber-Shirk, LW Lion (2014). “Flocculation-sedimentation performance model for laminar-flow hydraulic flocculation with polyaluminum chloride and aluminum sulfate coagulants”. Journal of Environmental Engineering 140 (3), 04014002

Kawamura, S. (1991). Integrated design of water treatment facilities, Wiley, New

York.

O'Melia, C. R. (1972). "Coagulation and flocculation." Chapter 2, Physico- chemical processes for water quality control, W. J. Weber, Jr., ed., Wiley-Interscience, New York.

Kawahigashi, Masayuki, et al. "Dissolved organic matter in small streams along a gradient from discontinuous to continuous permafrost." Global Change Biology 10.9 (2004): 1576-1586.

Österberg, R., I. Lindovist, and Kell Mortensen. "Particle size of humic acid." Soil Science Society of America Journal 57.1 (1993): 283-285.

Pennock, William. "Development Of The Turbulent Tube Flocculator." (2016).

Schulz, C. R., and Okun, D. A. (1984). Surface water treatment for com- munities in developing countries, Wiley, London.

Sharp, E.L., Jarvis, P., Parsons, S.A., Jefferson, B., 2006. Impact of fractional character on the coagulation of NOM. Colloid Surf. A 286, 104–111.

Shin, J. Y., Spinette, R. F., and O'Melia, C. R. (2008). "Stoichiometry of coagulation revisited." Environ. Sci. Technol., 42(7), 2582–2589.

Soh, Yeow Chong, Felicity Roddick, and John van Leeuwen. "The impact of alum coagulation on the character, biodegradability and disinfection by-product formation potential of reservoir natural organic matter (NOM) fractions." Water Science and Technology 58.6 (2008): 1173-1179.

Sun, Siwei, Monroe Weber-Shirk, and Leonard W. Lion. "Characterization of Flocs and Floc Size Distributions Using Image Analysis." Environmental engineering science 33.1 (2016): 25-34.

Swetland, K. A. (2012). “From stock to floc: An investigation into the physical/chemical processes controlling aluminum sulfate and polyalu- minum chloride behavior in a gravity powered drinking water treatment plant.” Ph.D. dissertation, Cornell Univ., Ithaca, NY.

Swetland, K. A., Weber-Shirk, M. L., and Lion, L. W. (2013). “Influence of polymeric Al-oxyhydroxide precipitate-aggregation on flocculation performance.” Environ. Eng. Sci., 30(9), 536–545.

Weber-Shirk, M. L. (2008). “An automated method for testing process parameters.” 〈https://confluence.cornell.edu/display/AGUACLARA/Process+Controller+Background〉 (May 01, 2012).

Weber-Shirk, M. L., and Lion, L. W. (2010). “Flocculation model and col- lision potential for reactors with flows characterized by high peclet numbers.” Water Res., 44(18), 5180–5187.

Willis, R. M. (1978). “Tubular settlers—A technical review.” J. Am. Water Works Assoc., 70(6), 331–335.